HHS Public Access

Author manuscript

Alcohol Clin Exp Res. Author manuscript; available in PMC 2023 August 01.

Published in final edited form as:

Alcohol Clin Exp Res. 2022 August ; 46(8): 1371–1383. doi:10.1111/acer.14893.

Mice lacking α4 nicotinic acetylcholine receptors are protected against alcohol-associated liver injury

Walter H. Watson, PhD[1,2], **Jeffrey D. Ritzenthaler**[3], **Edilson Torres-Gonzalez**[3], **Gavin E. Arteel, PhD**[4], **Jesse Roman, MD**[3]

[1]Department of Medicine, Division of Gastroenterology, Hepatology and Nutrition, University of Louisville, Louisville, KY

[2]Department of Pharmacology and Toxicology, University of Louisville, Louisville, KY

[3]Department of Medicine, Division of Pulmonary, Allergy and Critical Care Medicine and Jane & Leonard Korman Respiratory Institute, Thomas Jefferson University, Philadelphia, PA

[4]Department of Medicine, Division Gastroenterology, University of Pittsburgh, Pittsburgh, PA

Abstract

Background: Chronic alcohol abuse is a major risk factor for the development of liver steatosis, fibrosis and cirrhosis, but the mechanisms by which alcohol causes liver damage remain incompletely elucidated. This group has reported that α4 nicotinic acetylcholine receptors (α4 nAChRs) act as sensors for alcohol in lung cells. The purpose of the present study was to test the hypothesis that α4 nAChRs mediate the effects of alcohol in the liver.

Methods: Expression of acetylcholine receptor subunits in mouse liver was determined by RNA sequencing (RNA-seq). α4 nAChR knockout (α4 KO) mice were generated in C57BL/6J mice by introducing a mutation encoding an early stop codon in exon 4 of Chrna4, the gene encoding the α4 subunit of nAChRs. The presence of the inactivating mutation was established by polymerase chain reaction (PCR) and genomic sequencing, and the lack of α4 nAChR function was confirmed in primary fibroblasts isolated from the α4 KO mice. Wildtype (WT) and α4 KO mice were fed the Lieber-DeCarli diet (with 36% calories from alcohol) or pair fed an isocaloric maltose-dextrin control diet for a 6-week period that included a ramping up phase of increasing alcohol in the diet.

Results: Chrna4 was the most abundantly expressed nAChR subunit gene in mouse livers. After 6 weeks of alcohol exposure, WT mice had elevated serum transaminases and their livers showed increased fat accumulation, decreased Sirt1 protein levels, and accumulation of markers of oxidative stress and inflammation including Cyp2E1, Nos2, Sod1, Slc7a11, TNFα, and PAI1. All of these responses to alcohol were either absent or significantly attenuated in α4 KO animals.

Conclusion: Together, these observations support the conclusion that activation of α4 nAChRs by alcohol or one of its metabolites is one of the initial events promoting accumulation of excess fat and expression of inflammatory mediators. Thus, α4 nAChRs may represent viable targets for intervention in chronic alcohol-related liver disease.

Correspondence: Jesse Roman, MD, Jane & Leonard Korman Respiratory Institute, 211 South 9th Street, Suite 401, Philadelphia, PA 19107, Tel. 215-955-1671, Fax. 215-503-2995, jesse.roman@jefferson.edu, Walter H. Watson, PhD, University of Louisville – Medicine, 505 S. Hancock Street, Louisville, KY 40292, Tel. 502-852-4905, whwats01@louisville.edu.

Keywords

Fatty liver; Sirt1; nicotinic receptors; steatosis; alcohol

INTRODUCTION

Globally, alcohol use represents the most common substance use disorder, with 2.4 billion people actively consuming alcohol in 2016 (Thursz et al., 2019). The liver is a major target of alcohol toxicity. Alcohol-associated liver disease (ALD) is a spectrum of disorders ranging from simple steatosis to steatohepatitis, fibrosis, and cirrhosis (Hosseini et al., 2019). Hepatic fat accumulation (steatosis) represents one of the earliest pathological responses to chronic alcohol intake. Increased rates of lipid synthesis (lipogenesis) and decreased rates of lipid breakdown (e.g., fatty acid β-oxidation) both contribute to the accumulation of fat within hepatocytes in response to alcohol exposure (Jeon and Carr, 2020). Several genes that control lipogenesis are upregulated by activation of the transcription factor Srebp1 by alcohol (Jeon and Carr, 2020). Moreover, alcohol inhibits β-oxidation of fatty acids by inhibiting Pparα (Meng et al., 2020). There is evidence for crosstalk between the pathways regulating lipogenesis and β-oxidation. Indeed, both of these pathways are regulated by Sirt1, a protein deacetylase that is emerging as a master regulator of alcohol's effects on hepatic lipid metabolism (You et al., 2015, Ding et al., 2017). It is not entirely clear, however, how alcohol exposure inhibits Sirt1 expression and activity.

Alcohol exposure produces oxidative stress by increasing production of oxidants and depleting antioxidants. Sources of oxidants include CYP2E1-mediated alcohol metabolism and inflammatory cell activation (Beier et al., 2011, Kirpich et al., 2019). Kupffer cells, hepatic stellate cells, hepatocytes, and endothelial cells are sensitive to oxidative stress, which results in lipid peroxidation and damage to proteins and DNA. Under these circumstances, redox homeostasis is maintained by antioxidant mechanisms involving the activation of antioxidant enzymes such as catalase and superoxide dismutases and the generation of the non-enzymatic antioxidant glutathione (GSH) (Li et al., 2015). Oxidative stress also triggers changes in the expression and activity of lipid metabolism genes, the secretion of pro-inflammatory cytokines (e.g., tumor necrosis factor-α), alterations in fibrinolysis (e.g., plasminogen activator inhibitor −1), and surface expression of amino acid transporters (e.g., Slc7a11), among other changes. Because oxidative stress is an early consequence of alcohol toxicity that can exacerbate liver injury, identifying cellular mechanisms responsible for sensing and responding to alcohol may lead to novel ways to intervene and break this vicious cycle.

Previously, we showed that α4 nicotinic acetylcholine receptors (α4 nAChRs) act as alcohol sensors in mouse lung fibroblasts. Both pharmacological inhibitors and downregulation of α4 nAChR by siRNA inhibited the alcohol-induced expression of fibronectin in these cells (Ritzenthaler et al., 2013, Roman et al., 2005). These nAChRs are members of a family of non-selective cation channels that are activated by the neurotransmitter acetylcholine and are widely expressed at synaptic junctions (Lindstrom et al., 1996, Lindstrom, 1997). Non-neuronal cells and tissues also express some members of this family, and there is

abundant evidence that these receptors have a function outside of the central and peripheral nervous systems (Aistrup et al., 1999, Davis and de Fiebre, 2006, Zhang et al., 2017, Hiemke et al., 1996, Mizuno et al., 1982, Davies et al., 1982, Kishibe et al., 2015, Zia et al., 1997, Maus et al., 1998, Zheng et al., 2007). Sixteen genes encoding for nAChR subunits have been identified in mammals including nine distinct α subunits (α1-α7, α9 and α10), four β subunits (β1-β4), and the δ, γ and ε subunits (Pedersen et al., 2019). Except for nAChRs located at somatic neuromuscular junctions and in embryonic and denervated skeletal muscle, nAChRs assemble as hetero-pentamers containing combinations of α and β subunits. The α7 and α9 subunits can also form functional homo-pentamers (Pan et al., 2019).

In a recent analysis of data from several large genetic consortiums, it was found that human liver expresses high levels of Chrna4, the gene that encodes the α4 subunit of nAChRs, and that the tissue distribution of expression of Chrna4 and associated epigenetic markers were conserved between humans and mice (Zhang et al., 2017). An examination of CAGE-seq data revealed that hepatocytes, but not hepatic sinusoid or stellate cells, were responsible for the high liver expression of Chrna4 (Zhang et al., 2017). Despite its high level of expression, the function of Chrna4-encoded α4 nAChRs in the liver is unknown. To begin to address this gap in knowledge, we generated mice with an α4 nAChR knockout mutation. Herein, we describe the characterization of these animals, explore the impact of alcohol intake using a well-studied experimental model of alcohol-related liver disease, and examine the potential role of Sirt1 (You et al., 2015).

MATERIALS AND METHODS

Reagents

All reagents were purchased from Sigma Chemicals (St. Louis, MO) or Fisher Scientific (Pittsburgh, PA) unless otherwise specified.

Generation of α4 nAChR knockout mice

The α4 nAChR knockout animals were generated at the Transgenic Mouse Facility, University of California (Irvine, CA) using Crispr/Cas9 and SgRNA (CCCATCTGAACTCATCTGGGG) to target specific sequences and to generate a Double Strand Break (DSB) in exon 4 of the α4 nAChR gene in C57BL/6N mice. Genomic DNA was isolated and submitted to the University of California-Irvine sequencing core facility to verify the mutation; a 17 bp deletion introduced a premature Stop codon in exon 4. The α4 nAChR knockout animals (F1) were then backcrossed with wild type C57BL/6J mice (Jackson Laboratories, Bar Harbor, ME) for a minimum of 8 generations. All animals were housed in a pathogen-free facility with a 12-hour light/dark cycle and access to food and water ad libitum prior to initiation of liquid alcohol diets (see below). The institutional animal care and use committee (IACUC) at the University of Louisville approved all experiments.

Genotyping of homozygous and heterozygous α4 nAChR knockout mice

To distinguish between wild type (WT) and mutant alleles of the Chrna4 gene, we developed an amplification refractory mutation system (Newton et al., 1989) which we refer to as the Refractory Oligonucleotide Mutational Alpha4 Notification System (ROMANS) (see Figure 1B). Genomic DNA was isolated using the Phire Animal Tissue Direct PCR Kit (Thermo Scientific, Pittsburgh, PA). Genomic DNA was amplified by PCR using either the wildtype forward primer (5' ACTACA AACTGCGCTGGGACCC) or mutant forward primer (5' ACTACA AACTGCGCTGGGAATG) along with the reverse primer (5' TGGAAGAGTTTAAGGATGGGACC) of the ROMANS (see Figure 1B). Reactions were performed using the following parameters: 98 °C for 30 sec followed by 40 cycles of 98 °C for 5 s, 65 °C for 5 s, 72 °C for 10 s. Samples were loaded onto a 1% agarose gel, electrophoresed for 1 h at 150 volts in 1x TAE running buffer, and stained with ethidium bromide.

Chronic alcohol exposure

Male and female C57BL/6J WT mice obtained from Jackson Laboratories, and male and female mice homozygous for the α4 knock out mutation (α4 KO) were from our breeding colony of homozygous mice as described above. WT and α4 KO mice were exposed to chronic alcohol using the Lieber-DeCarli isocaloric liquid diets (Dyets, Inc., Bethlehem, PA) containing either ethanol (EtOH) or an isocaloric maltose-dextrin control diet (MD) according to the manufacturer's instructions. Diets were replaced daily using clean feeding tubes. The dietary period included the following exposure schedule: 0% v/v ethanol (days 1–2); 1% v/v ethanol (days 3–4); 2% v/v ethanol (days 5–6); 4% v/v ethanol (days 7–13); 5% v/v ethanol (days 14–20); 6% v/v ethanol (days 21–42). The 6% v/v ethanol results in 36% of the total calories derived from ethanol. Pair feeding was used to ensure that equal volumes of the liquid diets and, therefore, the same number of calories, were consumed by both groups.

Isolation and measurement of mRNA by qPCR

RNA was isolated from mouse liver tissue. Briefly, the liver tissue was harvested and placed into a sterile DNA- and RNA-free tube containing 1.4 mm ceramic beads (Omni International, Kennesaw, GA) and 700 ul Ribozol RNA isolation reagent (Amresco, Solon, OH). Samples were homogenized for 30 sec using a BeadMill 4 (Fisher Scientific, Hampton, NH) and centrifuged (10,000 x g) for 5 min. RNA was isolated from the supernatant and purified using Zymo Direct-ZOL RNA mini-prep plus (Zymo, Irvine, CA). The purified RNA was quantified using a Beckman Coulter DU800 spectrophotometer. RNA was reverse transcribed using the Bio-Rad iScript cDNA synthesis kit (Bio-Rad, Hercules, CA). Real-time quantitative PCR (qPCR) was performed for the quantification of Slc7a11, Tnf, Serpine1, Chrna4, Chrna7, Sod1, Nos2, B2m and Gapdh mRNA expression using TaqMan Gene Expression Assay (Slc7a11, Mm00442530_m1; Tnf, Mm00443258_m1; Serpine1, Mm00436753_m1; Chrna4, Mm00516561; Chrna7, Mm01312230_m1; Sod1, Mm01344233_g1; Nos2, Mm00440502_m1; B2m, Mm00437762_m1; Gapdh, Mm99999915_g1; Life Technologies, Carlsbad, CA) according to the manufacturer's instructions. The StepOnePlus Real Time

PCR System (Life Technologies, Carlsbad, CA) was used with the following reaction settings: 50 °C for 2 min, 95 °C for 0 min, followed by 40 cycles of 95 °C for 15 s and 60 °C for 1 min. Results were analyzed using StepOnePlus Software version 2.3 and the amplification curves were subjected to the mathematical equation of the second derivative. Ct values were normalized to the housekeeping gene B2m. Results were expressed as the fold increase in mRNA compared to samples from WT pair-fed mice using the 2-ΔΔCt method.

Isolation and measurement of liver protein

Protein was isolated from mouse liver tissue. Briefly, liver tissue was placed into a 2 ml bead tube containing 1.4 mm ceramic beads (Omni International, Kennesaw, GA) and RIPA buffer (Thermofisher, Waltham, MA) and homogenized using a Bead Mill 4 cell disruptor (Thermofisher, Waltham, MA). The total protein concentration was measured using Bradford protein dye reagent (Bio-Rad, Hercules, CA) and quantified using a Beckman DU800 spectrophotometer (Beckman Coulter, Brea, CA) at OD 595. Samples (25 μg) were mixed with sample buffer (2x, 100 mM Tris pH 6.8, 4 % SDS, 0.2% Bromophenol Blue, 20% Glycerol), heated to 98°C for 5 min, centrifuged and loaded onto a 10% SDS polyacrylamide gel and electrophoresed at 150 V for 1 hour. Afterwards, protein was transferred onto 0.2 μm nitrocellulose membrane (Bio-Rad, Hercules, CA) at 25V for 1.5 hour using a Trans-Blot SD semi-dry transfer cell (Bio-Rad, Hercules, CA). Membranes were blocked for 45 min at room temperature in block buffer (Odyssey, Li-COR Biosciences, Lincoln, NE). Membranes were then incubated with primary antibody against GAPDH (Abcam, #ab8245, 1:5000), Beta-actin (Abcam, #ab8224, 1:5000 dilution), Slc7a11 (Abcam, #175186, 1:1000 dilution), Tnf (Cell Signaling #11948, 1:1000 dilution), Cyp2E1 (Abcam, #ab28146, 1:1000 dilution), or Sirt1 (Cell Signaling, #9475, 1:1000 dilution) overnight at 4ºC. Membranes were washed (3 × 10 min) with phosphate buffered saline (PBS) solution containing 0.2% tween-20 (PBST) and incubated with secondary antibody (LI-COR, goat anti rabbit, #926–32211, #926–68071 or goat anti-mouse, #926–68070, #926–32210 at 1:5000 or 1:20000 dilution) for 1 hour at room temperature. Membranes were washed again in PBST (3 × 10 min) and scanned using a LI-COR Odyssey CLx imaging system and analyzed in Image Studio Lite (LI-COR).

Analysis of nAChR subunit expression

As part of a separate study (Young et al., 2019), male and female WT C57BL/6J mice were fed a purified diet providing 13% of calories from fat (TD.16377, Envigo, Madison, WI) beginning at weaning and continuing for 10 weeks. RNA was isolated from the livers and analyzed by RNA-seq. Fragments per kilobase of exon per million reads mapped (FPKM) were determined for each of the nAChR subunits.

Derivatization and HPLC analysis of plasma and liver tissue

Mouse plasma and liver tissue were analyzed for levels of cysteine (Cys), cystine (CySS), GSH, glutathione disulfide (GSSG), and cysteine-glutathione disulfide (CySSG) by HPLC. Briefly, deproteinized plasma and tissue samples were derivatized by the successive addition of iodoacetic acid and dansyl chloride, and analyzed by HPLC (Waters Corporation, Millford, MA) as previously described (Jones and Liang, 2009, Watson et al., 2020).

Concentrations of Cys, CySS, GSH, GSSG, CySSG were measured by integration relative to the internal standard γ-glutamyl glutamate. Total glutathione was calculated by the equation: Total GSH = [GSH] + 2*[GSSG] + [CySSG].

Measurement of ALT and AST liver enzymes

Serum Alanine Aminotransferase (ALT) and Aspartate Aminotransferase (AST) enzyme levels were measured by Colorimetric Detection using kits from Sigma (AST, #MAK055; ALT, #MAK052, St. Louis, MO). All results were recorded as the amount of activity in U/L by comparison to a standard curve.

Histological analysis and Oil Red O staining

Liver tissues were harvested and fixed with formalin, processed, and embedded in paraffin. Afterwards, tissue sections were cut using a Leica microtome (Leica, Wetzlar, Germany) at a thickness of 6 μm and stained using standard procedures for hematoxylin and eosin (H&E) (Fisher, Pittsburgh, PA). A portion of liver tissue was also harvested and immediately flash-frozen in liquid nitrogen for staining with Oil Red O. The frozen tissue was embedded in Tissue-Tek OCT using standard tissue molds. The frozen liver tissue was sectioned using a cryotome and placed on glass slides. Sections were incubated with Oil Red O staining solution for 10 min at room temperature. Afterwards, tissue sections were counterstained with hematoxylin and photographed.

Measurement of hepatic triglycerides and free fatty acids

Liver triglyceride (TG) and free fatty acid (FFA) levels were determined using commercial kits according to the manufacturer's instructions (Thermo Scientific) (Li et al., 2020).

Myeloperoxidase staining

Mouse livers were fixed in buffered formalin (Fisher Scientific, Waltham, MA) overnight at room temperature, dehydrated and embedded in paraffin. Six μm sections were deparaffinized and rehydrated, and antigen retrieval was performed using sodium citrate (pH 6). Sections were stained with an antibody to myeloperoxidase (ab208670 from Abcam, Waltham, MA) at a dilution of 1:500. Images were taken using an EVOS FL microscope (Life Technologies, Carlsbad, CA) at 20X magnification. Three mice from each group were analyzed. For each mouse, ten fields were randomly selected, and cells positive for myeloperoxidase were counted in each field. The average number of positive cells per field for each mouse was used to compare groups in GraphPad Prism.

Determination of alcohol metabolism rates

Five female and five male WT and α4 KO mice were given a bolus i.p. injection of alcohol (1.12 g/kg body weight) and blood was collected 0.5, 1 and 2 hours later. Blood alcohol concentrations were measured with the EnzyChrom Ethanol Assay Kit (BioAssay Systems) following the manufacturer's instructions. Concentration vs time data were fit to a linear model reflecting zero order metabolism of alcohol.

Analysis of data and statistical evaluation

All assays were performed on at least 4 and up to 24 biological replicates for each sample group. Numerical data are presented as means plus standard error of the mean. Significance was assessed by 2-way ANOVA using Tukey's multiple comparison test in GraphPad Prism to compare individual groups. For graphical representation of significance between groups, the following notations were used: $p<0.0332$ (*), $p<0.0021$ (**), $p<0.0002$ (***), and $p<0.0001$ (****).

RESULTS

Expression of nicotinic acetylcholine receptor subunits in murine liver

To begin to understand the spectrum of nAChRs expressed in mouse liver, we analyzed RNA-seq data that we obtained from the livers of male and female mice fed a low fat control diet as part of another study (Young et al., 2019). As shown in Figure 1A, the gene encoding the α4 subunit (Chrna4) was by far the most abundantly expressed. Chrna2 (α2) was also expressed, but all other α subunits were expressed at very low levels or not at all. Among the potential α4 nAChR binding partners, both β1 and β2 were expressed in mouse liver (Figure 1A). Male and female mice had similar patterns of expression of the nAChR subunits in that study.

Generation of α4 nAChR knockout mice

Given that Chrna4 is abundantly expressed in the liver, we reasoned that it might play a functional role in this non-neuronal tissue and that its absence could alter alcohol-related effects. To test this idea, we generated α4 nAChR (Chrna4) knockout mice (α4 KO) using Crispr/Cas technology and confirmed the mutation of both alleles by PCR (Figure 1B). Mice with null mutations in the α4 nAChR subunit appeared normal and healthy, which is consistent with observations by others (Marubio et al., 2003, Cordero-Erausquin et al., 2000). The α4 KO animals developed normally and their phenotype was indistinguishable from C57BL/6J mice. Both male and female α4 KO mice were fertile and had body weights comparable to similarly aged WT C57BL/6J mice. Mating of the α4 KO animals produced litter sizes of 6 to 9 pups, similar to that of the C57BL/6J mice. Histological examination of lung and liver demonstrated normal tissue structure, and other abdominal organs in both male and female α4 KO animals appeared normal upon macroscopic examination. The knock out effectively prevented expression of the Chrna4 gene in both male and female mice, as evidenced by the lack of detectable mRNA by qPCR (Figure 1C). In WT mice, Chrna4 was expressed at higher levels in the livers of female mice on the control liquid diet used in the present study (Figure 1C), confirming that the higher levels seen by RNA-seq in female mice (Figure 1A) was reproducible and consistent from the low fat diet to the high fat diet used in the 2 studies.

Alcohol increases Chrna4 expression, fat accumulation, injury and inflammation in the livers of WT animals, but not in α4 KO animals

To study the impact of alcohol, wildtype (WT) and α4 KO mice were fed the Lieber-DeCarli diet (with 36% calories from alcohol) or pair fed an isocaloric maltose-dextrin control diet

for 6 weeks. The results of assays presented in the subsequent figures were performed on samples from male mice. Some assays were also performed on samples from female mice, and the results of these studies are included in the Supporting Information, as they suggest that similar mechanisms are relevant in females, but further investigations are needed. Chrna4 mRNA levels were increased in the livers of alcohol-fed WT mice but remained undetectable in α4 KO mice (Figure 2A and Figure S1). Chrna7, the gene encoding the α7 subunit, was undetectable in either WT or α4 KO mice, regardless of whether they received the alcohol diet or the maltose-dextrin control diet (not shown). To provide evidence that hepatocytes express α4 nAChRs, Chrna4 expression was also measured in AML12 mouse hepatocytes with and without alcohol exposure. Chrna4 was expressed in these cells, and alcohol exposure increased mRNA levels, similar to what was seen in vivo (Figure 2B). In contrast, the levels for Chrna7 (another nAChR) were undetectable in AML12 cells, even after exposure to alcohol (Figure 2C). To determine whether mice lacking Chrna4 had altered alcohol metabolism, WT and α4 KO mice were challenged with a single i.p. injection of alcohol, and blood alcohol concentrations were monitored over the next 2 hours. The alcohol exposure resulted in similar peak concentrations and rates of clearance in WT and α4 KO mice of both sexes (Figure 2D; **See** Figure S2 **for data in females**).

H&E staining showed that WT and α4 KO mice had normal histology when pair fed the MD diet. Upon exposure to alcohol, WT mice showed evidence of steatosis in the form of empty vacuoles (Figure 3A and Figure S3A). Oil Red O staining, which stains neutral lipids red, confirmed that the alcohol diet increased lipid levels in female and male WT mice, and that α4 KO mice were protected against lipid accumulation (Figure 3B and Figure S3B). In contrast, none of the alcohol-associated changes seen in the WT mice were observed in the α4 KO mice. Additional evidence of steatosis was provided by direct measurement of hepatic triglycerides (Figure S3C) and free fatty acids (Figure S3D). These data demonstrate that triglycerides, but not free fatty acids, were elevated in the livers of female WT mice exposed to alcohol, consistent with previous reports (Lu et al., 2008). We did not measure lipids in male mice, but others have shown the same pattern of elevated triglycerides and normal free fatty acids in male mice fed a liquid alcohol diet (Kirpich et al., 2012). Taken together, these results suggest that the presence of α4 nAChRs is required for alcohol-induced hepatic steatosis.

To determine whether α4 KO mice are protected from alcohol-induced hepatocyte cell death, we measured circulating levels of liver transaminases. Alcohol exposure resulted in a 2-fold elevation in plasma AST and ALT in WT mice, while α4 KO mice showed no increase (Figure 4A-B). Both of these enzymes were higher in the MD pair fed α4 KO mice compared to MD pair fed WT mice, but alcohol had no additional effect in the α4 KO mice. Alcohol exposure also increased expression of inflammatory mediators in the liver. Hepatic TNFα and PAI-1 mRNA levels were increased in WT mice, but not in the α4 KO mice (Figure 4C-D). Protein levels of TNFα were also increased by alcohol in the livers of WT mice, but not in α4 KO mice (Figure 4E).

Effects of alcohol and α4 nAChRs on markers of oxidative stress

Superoxide dismutase (Sod1) and inducible nitric oxide synthase (Nos2) have been shown to be elevated in response to chronic alcohol intake and can contribute to the formation of hydrogen peroxide, nitric oxide and peroxynitrite (McKim et al., 2003). Both enzymes were increased at the mRNA level in the livers of WT mice in response to alcohol, but alcohol did not alter the expression of these genes in the α4 KO mice (Figure 5A-B and Figure S4). We also examined the effect of alcohol and α4 KO on liver glutathione. GSH is the major intracellular thiol antioxidant (Halvey et al., 2005, Watson et al., 2003), and GSH depletion in response to alcohol is indicative of oxidative stress (Tsukamoto and Lu, 2001). Our studies revealed that the livers of α4 KO mice had higher levels of total GSH than WT mice. Alcohol did not significantly affect hepatic total GSH in either strain (Figure 5C). These observations led us to examine the expression of Slc7a11, the xCT subunit of the system Xc^- transporter, which imports cystine to support glutathione synthesis (Sato et al., 2000). Alcohol exposure increased Slc7a11 expression in WT mice, consistent with an increased demand for the rate-limiting amino acid for GSH synthesis. Alcohol feeding had no effect on Slc7a11 mRNA levels in the liver of α4 KO mice (Figure 5D). Slc7a11 expression was higher in α4 KO mouse livers than in WT mice pair-fed the maltose-dextrin control diet, but this did not reach statistical significance (Figure 5D). There was also no difference in Slc7a11 protein levels between WT and α4 KO mice on the maltose-dextrin control diet (Figure 5E). Alcohol increased Slc7a11 at the protein level in the WT, but not in the α4 KO mice (Figure 5E). One source of reactive oxygen species in mice fed alcohol is Cyp2E1, an enzyme that metabolizes alcohol and that is upregulated upon chronic exposure. The protein levels were indeed increased in WT mice fed alcohol, but this was not observed in the α4 KO mice (Figure 5F). Taken together, these results suggest that alcohol-induced oxidative stress is limited in the livers of α4 KO mice.

Immune cell infiltration was not increased by alcohol in this model

Myeloperoxidase (MPO) staining of liver slices was used to gauge the recruitment and activation of inflammatory cells (Figure 6A). There were no statistical differences in the number of MPO positive cells in the livers of mice from any of the 4 treatment groups (Figure 6B).

α4 nAChRs mediate alcohol-related decrease in Sirt1 expression

Several studies suggest that lipid accumulation in liver in response to alcohol is mediated through effects on Sirt1 (Trepiana et al., 2018). Sirt1 is a deacetylase that works in conjunction with AMPK to sense and respond to changing energy demands. Among its downstream targets are regulators of lipogenesis and fatty acid β-oxidation. Thus, Sirt1 is a master regulator of lipid homeostasis in the liver. As shown in Figure 7, alcohol exposure decreased Sirt1 protein levels in WT liver, but not in α4 KO mice.

DISCUSSION

ALD affects millions worldwide with liver steatosis representing the earliest pathological response to chronic alcohol intake. Previous work in our laboratory pointed to α4 nAChRs as sensors of alcohol in lung, which prompted our current work further supporting an

important role for α4 nAChRs in mediating the detrimental effects of alcohol in liver. This work focused on *in vivo* experiments performed in animals exposed to alcohol. First, we found that the gene encoding the α4 subunit was expressed in mouse liver, and it was upregulated in response to chronic alcohol feeding. Under such circumstances, WT mice exhibited the characteristic increase in hepatic fat accumulation. There was also evidence of mild oxidative stress in the WT mice fed alcohol, as well as increased expression of Sod1 and Nos2, but no decrease in GSH. The data suggested that cell death and inflammation were mild in our model. Although hepatic expression of TNFα and PAI1 were increased in response to alcohol in the WT mice, there was no evidence for increased neutrophil infiltration. Finally, we observed that the alcohol-induced steatosis in WT mice was accompanied by downregulation of Sirt1, a master regulator lipid metabolism in the liver. The combination of excess lipids and oxidative stress can contribute to inflammation and cell death. In contrast to WT mice, the alcohol-induced changes described, including the mild signs of oxidative stress and inflammation detected, were not seen in the α4 KO mice. In essence, all of the effects of alcohol noted were prevented by knocking out the gene encoding the α4 subunit of nAChRs, suggesting that it is playing a proximal role in mediating the hepatoxicity of alcohol (see Figure 8). To our knowledge, this is one of the first studies to implicate nAChRs in alcohol-related liver toxicity, and the first to implicate α4 nAChRs in mediating alcohol-induced fat accumulation.

The mechanism by which α4 nAChRs mediate the effects of alcohol in liver is unknown. In earlier work, we reported that alcohol stimulates cultured lung fibroblast expression of fibronectin, a matrix glycoprotein implicated in lung injury and repair (Roman et al., 2005). In this simple *in vitro* model, we found that alcohol induced the activation of protein kinase C, induced cAMP accumulation, and promoted nuclear translocation and DNA binding of CREB. It is possible that alcohol triggers the influx of cations through α4 nAChRs as seen in other nAChRs, which activates downstream signaling ultimately affecting Sirt1 levels as observed in the current study. α4 KO mice could also be protected from the hepatotoxicity of alcohol if these mice metabolized alcohol more rapidly than their WT counterparts, but this does not appear to be the case. Peak blood alcohol concentrations and rates of alcohol clearance following an acute administration of alcohol were similar in WT and KO mice. Our study did not investigate whether alcohol metabolism is altered during chronic ingestion of alcohol in WT versus α4 KO mice. However, there are several observations presented in the literature that suggest that α4 nAChRs are not likely to affect alcohol consumption or metabolism in animals. First, Kamens et al., demonstrated that varenicline, a partial agonist of α4β2 nAChRs and less potent full agonist of α7 nAChRs, decreased ethanol consumption in mice, but this effect did not require the expression of α4β2 or α7 nAChRs (Kamens et al., 2010). They also reported that varenicline did not alter the clearance of alcohol, again suggesting that these receptors do not play important roles alcohol metabolism. Subsequent studies confirmed that varenicline does not alter alcohol metabolism in mice (Kamens et al., 2018). Another potential partner for α4 is β4. In similar experiments, animals deficient in β4 were shown to display no changes in ethanol consumption or blood alcohol levels at 30 min after alcohol presentation (Patkar et al., 2016). Thus, based on studies with nAChR knockout mice and pharmacological agents, the data available to date do not implicate α4β2 or α4β4 in alcohol consumption or metabolism. In a human study, subjects were

administered varenicline for 7 days to achieve steady state levels and then given a single priming dose of alcohol followed by an ad libitum period of alcohol consumption. Peak breath alcohol levels were not correlated with plasma varenicline concentrations following either the priming phase or the ad libitum phase of alcohol consumption, providing evidence that alcohol metabolism is not affected by α4β2 signaling in humans (Roberts et al., 2017).

Our studies did not determine which cell types within the WT liver express Chrna4, but a previous study suggested that hepatocytes express this subunit, whereas hepatic stellate cells and sinusoidal endothelial cells do not (Zhang et al., 2017). We found that Chrna4 knockout mice fail to downregulate Sirt1 in response to alcohol. Because Sirt1 expression within hepatocytes controls lipid metabolism, this suggests that expression of Chrna4 on hepatocytes is involved in sensing alcohol and mediating changes in signaling and function leading to accumulation of lipids within these cells. In support of this, we found that AML12 cells (an immortalized mouse hepatocyte cell line) expressed Chrna4 and that alcohol upregulated its expression in these cells. We attempted to use immunohistochemistry to identify specific cell types within the liver that express α4 nAChRs. Using 2 commercially available antibodies, we observed staining throughout the liver. However, the staining pattern was very similar in both WT and α4 KO mice (not shown). Thus, it was clear that this staining was non-specific. Although this work focuses on the liver, it is likely that alcohol affects other organs via α4 nAChRs. In unpublished work, we found that alcohol triggered the upregulation of certain inflammatory markers in the lungs of wildtype animals, but not in α4 KO mice. Further work directed at improving understanding about how these events mediate the effects of alcohol in distinct organs will require testing in tissue-specific α4 KO animals in relevant models. In addition, cell type-specific α4 KO mice will be needed to assess whether α4 nAChRs are expressed on other cell types such as Kupffer cells and cholangiocytes and contribute to the pathogenesis of alcohol-associated liver injury.

The presence of acetylcholine receptors in the liver implies that acetylcholine is being used as a signaling molecule in this tissue. It is unknown at this time whether termini of the vagus nerve that innervates the liver release acetylcholine to act upon receptors on hepatocytes or whether extracellular acetylcholine is being secreted by hepatocytes or some other cell type to act in an autocrine or paracrine manner to influence cells expressing acetylcholine receptors. Efferent signaling through the vagus nerve promotes anti-inflammatory and anti-apoptotic pathways in the liver (Hiramoto et al., 2008). These responses are likely mediated by Kupffer cells expressing α7 nAChRs (Li et al., 2018, Li et al., 2014). Mice lacking α7 nAChRs are more susceptible to liver injury induced by inflammatory stimuli, whereas the current study shows that mice lacking α4 nAChRs are protected from liver injury induced by alcohol. It appears that α4 and α7 nAChRs may activate opposing pathways in the liver.

The metabolism of alcohol yields products that are responsible for many of the adverse effects of alcohol (Teschke, 2018). Cyp2E1 is a microsomal alcohol metabolizing enzyme that is upregulated by alcohol and contributes to its toxicity, possibly by producing superoxide anion (Lu and Cederbaum, 2008). Alcohol dehydrogenase produces acetaldehyde and NADH, both of which have been linked to alcohol toxicity (Cederbaum, 2012, Watson et al., 2011, Arteel et al., 2003). In fibroblasts, metabolism of alcohol to acetaldehyde by alcohol dehydrogenase was required for the α4 nAChR-mediated

upregulation of fibronectin (Roman et al., 2005). It is not known whether it is alcohol itself or one of its metabolites that mediate the α4 nAChR-mediated effect on the liver reported here.

Increased production of superoxide and hydrogen peroxide by mitochondria and Cyp2E1 have been linked to decreased GSH levels in the livers of mice chronically exposed to alcohol (Tan et al., 2020), and glutathione depletion is known to contribute to the toxicity of alcohol in the liver (Gao and Bataller, 2011). GSH was not significantly depleted by alcohol in our WT mice, but α4 KO mice had higher hepatic GSH than WT mice, regardless of the diet they were fed. Of interest, no decrease in GSH was noted in our model. One explanation for the lack of GSH depletion could be that there was an increase in GSH production promoted by induction of SLc7a11 expression in the WT mice. Slc7a11 is the cystine transporter that supplies the rate-limiting amino acid for GSH synthesis, so we examined its expression to determine whether it was increased in α4 KO mice. There were no differences in Slc7a11 mRNA or protein between WT and α4 KO mice on the MD control diet. In response to alcohol, Slc7a11 levels were increased in WT mice but not in α4 KO mice. The former is consistent with a recent report that alcohol stimulates activity of Slc7a11 in mouse liver and primary mouse hepatocytes (Choi et al., 2019). In that study, alcohol-induced Slc7a11 upregulation was shown to activate adjacent hepatic stellate cells to promote lipid accumulation, and either genetic or pharmacological inhibition of Slc7a11 blocked the effect of alcohol on lipid accumulation (Choi et al., 2019). In our study, alcohol did not induce Slc7a11 expression in α4 KO mice. Additional research will be needed to determine the mechanisms by which α4 nAChRs regulate Slc7a11 expression and the relative roles of cystine import and glutamate export in hepatic responses to alcohol.

Markers of oxidative stress other than GSH depletion were increased by alcohol in our WT mice. Sod1, Nos2 and Cyp2E1 were increased by alcohol. Interestingly, none of these markers were increased in α4 KO mice. Whereas the increases in Sod1 and Nos2 could be viewed as secondary to superoxide production (in the case of Sod1) or inflammatory cell recruitment (in the case of Nos2), Cyp2E1 is believed to be a primary source of oxidant production upon chronic alcohol exposure. Alcohol stabilizes Cyp2E1, leading to its accumulation. As Cyp2E1 metabolizes alcohol, superoxide anion can be released (Lu and Cederbaum, 2008). Because Cyp2E1 protein levels did not change in response to alcohol in the α4 KO mice, it appears that α4 nAChRs contribute to the mechanism that stabilizes the protein.

The current work focuses on the effects of alcohol in liver. However, alcohol affects many tissues in the body, and some of those extrahepatic effects are known to contribute to liver injury. For example, stimulation of lipolysis in adipose tissue increases delivery of fatty acids to the liver (Zhao et al., 2015), and disruption of intestinal tight junctions results in release of bacterial components such as lipopolysaccharides that contribute to hepatic inflammation (Beier et al., 2011, Kirpich et al., 2012, Tsukamoto et al., 2001). We postulate that α4 nAChRs expressed on hepatocytes and perhaps other liver cells are responding to alcohol and signaling through the downregulation of Sirt1 and subsequent accumulation of lipids. However, effects on non-hepatic tissues by alcohol might have contributed to the observations made.

In summary, our data suggest that α4 nAChRs mediate alcohol-induced inflammation and fat accumulation in liver perhaps through induction of oxidative stress and downregulation of Sirt1. This, in turn, stimulates lipogenesis and decreases β-oxidation, thereby promoting steatosis and lipotoxicity (Figure 8). The observations reported here unveil a novel pathway that could be targeted to prevent or treat alcohol-associated liver disease in humans. Antagonists selective for α4-containing nAChRs may prove to be useful in combatting steatosis or steatohepatitis in subjects chronically ingesting alcohol. It is encouraging to note that whole body deletion of Chrna4 had no obvious effects on the health of mice and that systemic administration of agents targeting nAChRs have been used in humans (Gonzales et al., 2006). However, acute administration of nAChR antagonists produces muscle relaxation by acting at neuromuscular junctions. To be useful in combatting ALD, such drugs would need to be targeted to the liver. Alternatively, novel therapeutic agents could be developed that target differences in binding sites between alcohol and endogenous ligands of nAChRs.

Supplementary Material

Refer to Web version on PubMed Central for supplementary material.

ACKNOWLEGEMENTS

This work was supported in part by a grant from the University of Louisville School of Medicine and by a grant from the Jewish Heritage Fund for Excellence Research Enhancement Grant Program at the University of Louisville School of Medicine. The authors would like to thank Wenke Feng and Lihua Zhang for their assistance with the measurements of triglycerides and free fatty acids. The authors have no conflicts of interest to declare.

Sources of Support:

R01AA021978, 1P50AA024337, P20GM113226, R01HL147088, R35ES028373 and P30ES030283

Abbreviations:

α4 nAChRs	α4 nicotinic acetylcholine receptors
α4 KO	α4 nAChR knockout
α7 nAChRs	α7 nicotinic acetylcholine receptors
ALD	alcohol-associated liver disease
ALT	Alanine Aminotransferase
AST	Aspartate Aminotransferase
Cys	cysteine
CySS	cystine
CySSG	cysteine-glutathione disulfide
EtOH	ethanol
GSH	glutathione

GSSG	glutathione disulfide
H&E	hematoxylin and eosin
IACUC	institutional animal care and use committee
MD	isocaloric maltose-dextrin control diet
qPCR	Real-time quantitative PCR
ROMANS	Refractory Oligonucleotide Mutational Alpha4 Notification System
ROS	reactive oxygen species
WT	wild type

REFERENCES

Aistrup GL, Marszalec W, Narahashi T (1999) Ethanol modulation of nicotinic acetylcholine receptor currents in cultured cortical neurons. Mol. Pharmacol. 55:39–49. [PubMed: 9882696]

Arteel G, Marsano L, Mendez C, Bentley F, McClain CJ (2003) Advances in alcoholic liver disease. Best Pract. Res. Clin. Gastroenterol. 17:625–647. [PubMed: 12828959]

Beier JI, Arteel GE, McClain CJ (2011) Advances in alcoholic liver disease. Curr Gastroenterol Rep 13:56–64. [PubMed: 21088999]

Cederbaum AI (2012) Alcohol metabolism. Clin. Liver Dis. 16:667–685. [PubMed: 23101976]

Choi WM, Kim HH, Kim MH, Cinar R, Yi HS, Eun HS, Kim SH, Choi YJ, Lee YS, Kim SY, Seo W, Lee JH, Shim YR, Kim YE, Yang K, Ryu T, Hwang JH, Lee CH, Choi HS, Gao B, Kim W, Kim SK, Kunos G, Jeong WI (2019) Glutamate Signaling in Hepatic Stellate Cells Drives Alcoholic Steatosis. Cell Metab.

Cordero-Erausquin M, Marubio LM, Klink R, Changeux JP (2000) Nicotinic receptor function: new perspectives from knockout mice. Trends Pharmacol. Sci. 21:211–217. [PubMed: 10838608]

Davies BD, Hoss W, Lin JP, Lionetti F (1982) Evidence for a noncholinergic nicotine receptor on human phagocytic leukocytes. Mol. Cell. Biochem. 44:23–31. [PubMed: 7087960]

Davis TJ, de Fiebre CM (2006) Alcohol's actions on neuronal nicotinic acetylcholine receptors. Alcohol Res Health 29:179–185. [PubMed: 17373406]

Ding RB, Bao J, Deng CX (2017) Emerging roles of SIRT1 in fatty liver diseases. Int. J. Biol. Sci. 13:852–867.

Gao B, Bataller R (2011) Alcoholic liver disease: pathogenesis and new therapeutic targets. Gastroenterology 141:1572–1585. [PubMed: 21920463]

Gonzales D, Rennard SI, Nides M, Oncken C, Azoulay S, Billing CB, Watsky EJ, Gong J, Williams KE, Reeves KR, Varenicline Phase 3 Study G (2006) Varenicline, an alpha4beta2 nicotinic acetylcholine receptor partial agonist, vs sustained-release bupropion and placebo for smoking cessation: a randomized controlled trial. JAMA 296:47–55. [PubMed: 16820546]

Halvey PJ, Watson WH, Hansen JM, Go YM, Samali A, Jones DP (2005) Compartmental oxidation of thiol-disulphide redox couples during epidermal growth factor signalling. Biochem. J. 386:215–219. [PubMed: 15647005]

Hiemke C, Stolp M, Reuss S, Wevers A, Reinhardt S, Maelicke A, Schlegel S, Schroder H (1996) Expression of alpha subunit genes of nicotinic acetylcholine receptors in human lymphocytes. Neurosci. Lett. 214:171–174. [PubMed: 8878111]

Hiramoto T, Chida Y, Sonoda J, Yoshihara K, Sudo N, Kubo C (2008) The hepatic vagus nerve attenuates Fas-induced apoptosis in the mouse liver via alpha7 nicotinic acetylcholine receptor. Gastroenterology 134:2122–2131. [PubMed: 18439427]

Hosseini N, Shor J, Szabo G (2019) Alcoholic Hepatitis: A Review. Alcohol Alcohol. 54:408–416. [PubMed: 31219169]

Jeon S, Carr R (2020) Alcohol effects on hepatic lipid metabolism. J. Lipid Res. 61:470–479. [PubMed: 32029510]

Jones DP, Liang Y (2009) Measuring the poise of thiol/disulfide couples in vivo. Free Radic. Biol. Med. 47:1329–1338. [PubMed: 19715755]

Kamens HM, Andersen J, Picciotto MR (2010) Modulation of ethanol consumption by genetic and pharmacological manipulation of nicotinic acetylcholine receptors in mice. Psychopharmacology 208:613–626. [PubMed: 20072781]

Kamens HM, Silva C, Peck C, Miller CN (2018) Varenicline modulates ethanol and saccharin consumption in adolescent male and female C57BL/6J mice. Brain Res. Bull. 138:20–25. [PubMed: 28778837]

Kirpich IA, Feng W, Wang Y, Liu Y, Barker DF, Barve SS, McClain CJ (2012) The type of dietary fat modulates intestinal tight junction integrity, gut permeability, and hepatic toll-like receptor expression in a mouse model of alcoholic liver disease. Alcohol. Clin. Exp. Res. 36:835–846. [PubMed: 22150547]

Kirpich IA, Warner DR, Feng W, Joshi-Barve S, McClain CJ, Seth D, Zhong W, Zhou Z, Osna NA, Kharbanda KK (2019) Mechanisms, biomarkers and targets for therapy in alcohol-associated liver injury: From Genetics to nutrition: Summary of the ISBRA 2018 symposium. Alcohol 83:105–114. [PubMed: 31129175]

Kishibe M, Griffin TM, Radek KA (2015) Keratinocyte nicotinic acetylcholine receptor activation modulates early TLR2-mediated wound healing responses. Int. Immunopharmacol. 29:63–70. [PubMed: 26071220]

Li DJ, Liu J, Hua X, Fu H, Huang F, Fei YB, Lu WJ, Shen FM, Wang P (2018) Nicotinic acetylcholine receptor alpha7 subunit improves energy homeostasis and inhibits inflammation in nonalcoholic fatty liver disease. Metabolism 79:52–63. [PubMed: 29129819]

Li F, Zhao C, Shao T, Liu Y, Gu Z, Jiang M, Li H, Zhang L, Gillevet PM, Puri P, Deng ZB, Chen SY, Barve S, Gobejishvili L, Vatsalya V, McClain CJ, Feng W (2020) Cathelicidin-related antimicrobial peptide alleviates alcoholic liver disease through inhibiting inflammasome activation. J. Pathol. 252:371–383. [PubMed: 33245573]

Li S, Tan HY, Wang N, Zhang ZJ, Lao L, Wong CW, Feng Y (2015) The Role of Oxidative Stress and Antioxidants in Liver Diseases. Int. J. Mol. Sci. 16:26087–26124.

Li Y, Xu Z, Yu Y, Yuan H, Xu H, Zhu Q, Wang C, Shi X (2014) The vagus nerve attenuates fulminant hepatitis by activating the Src kinase in Kuppfer cells. Scand. J. Immunol. 79:105–112. [PubMed: 24313447]

Lindstrom J (1997) Nicotinic acetylcholine receptors in health and disease. Mol. Neurobiol. 15:193–222. [PubMed: 9396010]

Lindstrom J, Anand R, Gerzanich V, Peng X, Wang F, Wells G (1996) Structure and function of neuronal nicotinic acetylcholine receptors. Prog. Brain Res. 109:125–137. [PubMed: 9009699]

Lu Y, Cederbaum AI (2008) CYP2E1 and oxidative liver injury by alcohol. Free Radic. Biol. Med. 44:723–738. [PubMed: 18078827]

Lu Y, Zhuge J, Wang X, Bai J, Cederbaum AI (2008) Cytochrome P450 2E1 contributes to ethanol-induced fatty liver in mice. Hepatology 47:1483–1494. [PubMed: 18393316]

Marubio LM, Gardier AM, Durier S, David D, Klink R, Arroyo-Jimenez MM, McIntosh JM, Rossi F, Champtiaux N, Zoli M, Changeux JP (2003) Effects of nicotine in the dopaminergic system of mice lacking the alpha4 subunit of neuronal nicotinic acetylcholine receptors. Eur. J. Neurosci. 17:1329–1337. [PubMed: 12713636]

Maus AD, Pereira EF, Karachunski PI, Horton RM, Navaneetham D, Macklin K, Cortes WS, Albuquerque EX, Conti-Fine BM (1998) Human and rodent bronchial epithelial cells express functional nicotinic acetylcholine receptors. Mol. Pharmacol. 54:779–788. [PubMed: 9804613]

McKim SE, Gabele E, Isayama F, Lambert JC, Tucker LM, Wheeler MD, Connor HD, Mason RP, Doll MA, Hein DW, Arteel GE (2003) Inducible nitric oxide synthase is required in alcohol-induced liver injury: studies with knockout mice. Gastroenterology 125:1834–1844. [PubMed: 14724835]

Meng FG, Zhang XN, Liu SX, Wang YR, Zeng T (2020) Roles of peroxisome proliferator-activated receptor alpha in the pathogenesis of ethanol-induced liver disease. Chem. Biol. Interact. 327:109176.

Mizuno Y, Dosch HM, Gelfand EW (1982) Carbamycholine modulation of E-rosette formation: identification of nicotinic acetylcholine receptors on a subpopulation of human T lymphocytes. J. Clin. Immunol. 2:303–308. [PubMed: 6982902]

Newton CR, Graham A, Heptinstall LE, Powell SJ, Summers C, Kalsheker N, Smith JC, Markham AF (1989) Analysis of any point mutation in DNA. The amplification refractory mutation system (ARMS). Nucleic Acids Res. 17:2503–2516. [PubMed: 2785681]

Pan Z, Zhao M, Peng Y, Wang J (2019) Functional divergence analysis of vertebrate neuronal nicotinic acetylcholine receptor subunits. J. Biomol. Struct. Dyn. 37:2938–2948. [PubMed: 30044167]

Patkar OL, Belmer A, Tarren JR, Holgate JY, Bartlett SE (2016) The effect of varenicline on binge-like ethanol consumption in mice is beta4 nicotinic acetylcholine receptor-independent. Neurosci. Lett. 633:235–239. [PubMed: 27693436]

Pedersen JE, Bergqvist CA, Larhammar D (2019) Evolution of vertebrate nicotinic acetylcholine receptors. BMC Evol. Biol. 19:38. [PubMed: 30700248]

Ritzenthaler JD, Roser-Page S, Guidot DM, Roman J (2013) Nicotinic acetylcholine receptors are sensors for ethanol in lung fibroblasts. Alcohol. Clin. Exp. Res. 37:914–923. [PubMed: 23421903]

Roberts W, Verplaetse TL, Moore K, Oberleitner L, Picciotto MR, McKee SA (2017) Effects of varenicline on alcohol self-administration and craving in drinkers with depressive symptoms. J Psychopharmacol 31:906–914. [PubMed: 28351203]

Roman J, Ritzenthaler JD, Bechara R, Brown LA, Guidot D (2005) Ethanol stimulates the expression of fibronectin in lung fibroblasts via kinase-dependent signals that activate CREB. Am. J. Physiol. Lung Cell Mol. Physiol. 288:L975–987. [PubMed: 15653713]

Sato H, Tamba M, Kuriyama-Matsumura K, Okuno S, Bannai S (2000) Molecular cloning and expression of human xCT, the light chain of amino acid transport system xc. Antioxid. Redox Signal. 2:665–671. [PubMed: 11213471]

Tan HK, Yates E, Lilly K, Dhanda AD (2020) Oxidative stress in alcohol-related liver disease. World J. Hepatol. 12:332–349.

Teschke R (2018) Alcoholic Liver Disease: Alcohol Metabolism, Cascade of Molecular Mechanisms, Cellular Targets, and Clinical Aspects. Biomedicines 6.

Thursz M, Kamath PS, Mathurin P, Szabo G, Shah VH (2019) Alcohol-related liver disease: Areas of consensus, unmet needs and opportunities for further study. J. Hepatol. 70:521–530. [PubMed: 30658117]

Trepiana J, Milton-Laskibar I, Gomez-Zorita S, Eseberri I, Gonzalez M, Fernandez-Quintela A, Portillo MP (2018) Involvement of 5'-Activated Protein Kinase (AMPK) in the Effects of Resveratrol on Liver Steatosis. Int. J. Mol. Sci. 19.

Tsukamoto H, Lu SC (2001) Current concepts in the pathogenesis of alcoholic liver injury. FASEB J. 15:1335–1349. [PubMed: 11387231]

Tsukamoto H, Takei Y, McClain CJ, Joshi-Barve S, Hill D, Schmidt J, Deaciuc I, Barve S, Colell A, Garcia-Ruiz C, Kaplowitz N, Fernandez-Checa JC, Yokoyama H, Okamura Y, Nakamura Y, Ishii H, Chawla RK, Barve S, Joshi-Barve S, Watson W, Nelson W, Lin M, Ohata M, Motomura K, Enomoto N, Ikejima K, Kitamura T, Oide H, Hirose M, Bradford BU, Rivera CA, Kono H, Peter S, Yamashina S, Konno A, Ishikawa M, Shimizu H, Sato N, Thurman R (2001) How is the liver primed or sensitized for alcoholic liver disease? Alcohol. Clin. Exp. Res. 25:171S–181S. [PubMed: 11391068]

Watson WH, Chen Y, Jones DP (2003) Redox state of glutathione and thioredoxin in differentiation and apoptosis. BioFactors 17:307–314. [PubMed: 12897452]

Watson WH, Greenwell JC, Zheng Y, Furmanek S, Torres-Gonzalez E, Ritzenthaler JD, Roman J (2020) Impact of sex, age and diet on the cysteine/cystine and glutathione/glutathione disulfide plasma redox couples in mice. J. Nutr. Biochem. 84:108431.

Watson WH, Song Z, Kirpich IA, Deaciuc IV, Chen T, McClain CJ (2011) Ethanol exposure modulates hepatic S-adenosylmethionine and S-adenosylhomocysteine levels in the isolated perfused rat liver through changes in the redox state of the NADH/NAD(+) system. Biochim. Biophys. Acta 1812:613–618. [PubMed: 21296661]

You M, Jogasuria A, Taylor C, Wu J (2015) Sirtuin 1 signaling and alcoholic fatty liver disease. Hepatobiliary Surg Nutr 4:88–100. [PubMed: 26005675]

Young JL, Yan X, Xu J, Yin X, Zhang X, Arteel GE, Barnes GN, States JC, Watson WH, Kong M, Cai L, Freedman JH (2019) Cadmium and High-Fat Diet Disrupt Renal, Cardiac and Hepatic Essential Metals. Sci. Rep. 9:14675. [PubMed: 31604971]

Zhang B, Madden P, Gu J, Xing X, Sankar S, Flynn J, Kroll K, Wang T (2017) Uncovering the transcriptomic and epigenomic landscape of nicotinic receptor genes in non-neuronal tissues. BMC Genomics 18:439. [PubMed: 28583088]

Zhao C, Liu Y, Xiao J, Liu L, Chen S, Mohammadi M, McClain CJ, Li X, Feng W (2015) FGF21 mediates alcohol-induced adipose tissue lipolysis by activation of systemic release of catecholamine in mice. J. Lipid Res. 56:1481–1491. [PubMed: 26092866]

Zheng Y, Ritzenthaler JD, Roman J, Han S (2007) Nicotine stimulates human lung cancer cell growth by inducing fibronectin expression. Am. J. Respir. Cell Mol. Biol. 37:681–690. [PubMed: 17600315]

Zia S, Ndoye A, Nguyen VT, Grando SA (1997) Nicotine enhances expression of the alpha 3, alpha 4, alpha 5, and alpha 7 nicotinic receptors modulating calcium metabolism and regulating adhesion and motility of respiratory epithelial cells. Res. Commun. Mol. Pathol. Pharmacol. 97:243–262. [PubMed: 9387186]

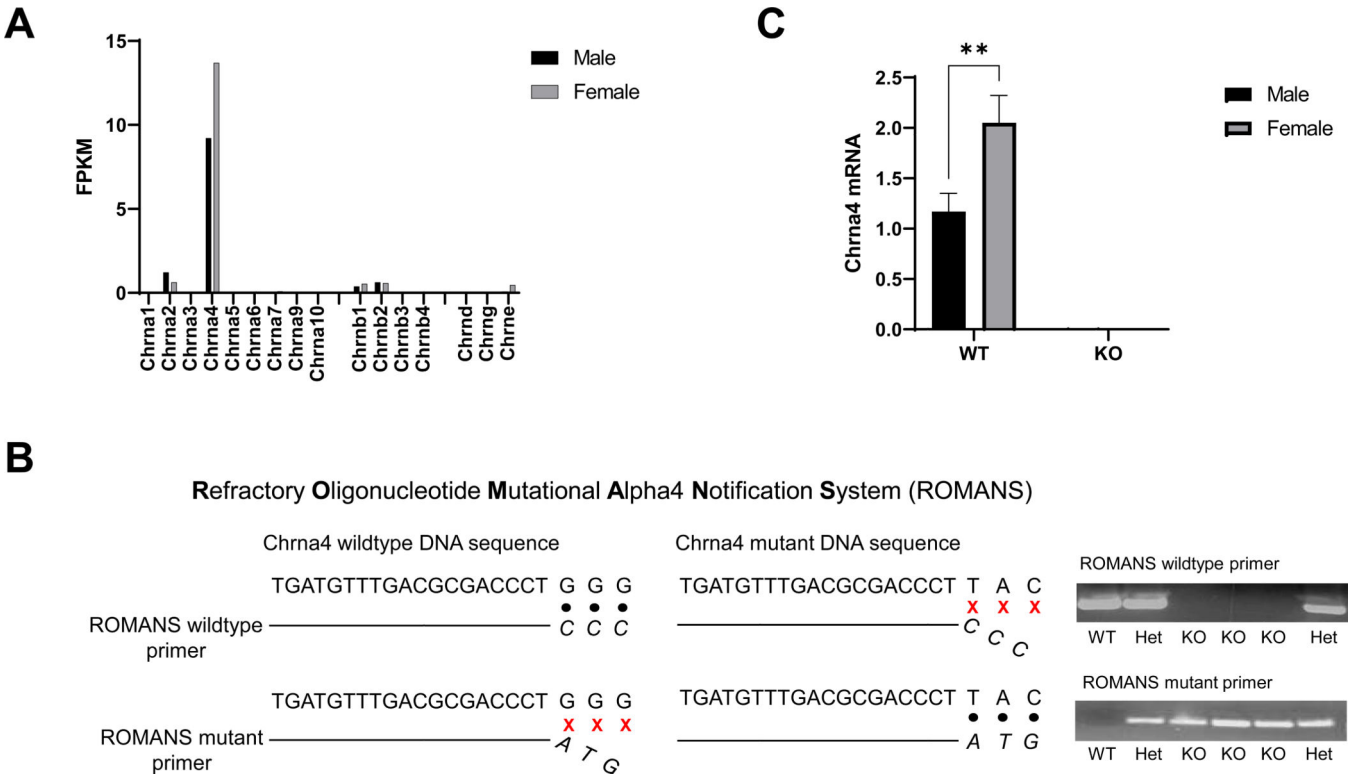

Figure 1. Nicotinic acetylcholine receptor subunit expression in male and female murine liver and generation of the α4 nAChR (Chrna4) knockout mouse.

(**A)** Nicotinic acetylcholine receptor subunit expression levels in mouse liver were estimated by FPKM from RNA-seq analysis. (**B)** Crispr/Cas9 technology was used to generate the α4 nAChR (Chrna4) knockout mouse and the resulting genetic mutation of both α4 nAChR alleles was confirmed with the use of the Refractory Oligonucleotide Mutational Alpha 4 Notification System (ROMANS). Agarose gel image of ROMANS PCR products using the wildtype or mutant primer along with the α4 nAChR reverse primer. Closed circle represents compatible base-pair, "X" represents mismatched base-pair. WT, wildtype allele; KO, α4 nAChR knockout allele; Het, heterozygous with both wildtype and α4 nAChR knockout alleles. (**C**) Chrna4 mRNA levels were measured by qPCR in male WT and α4 KO mice. ** - $p<0.005$ by unpaired 2-tailed t test.

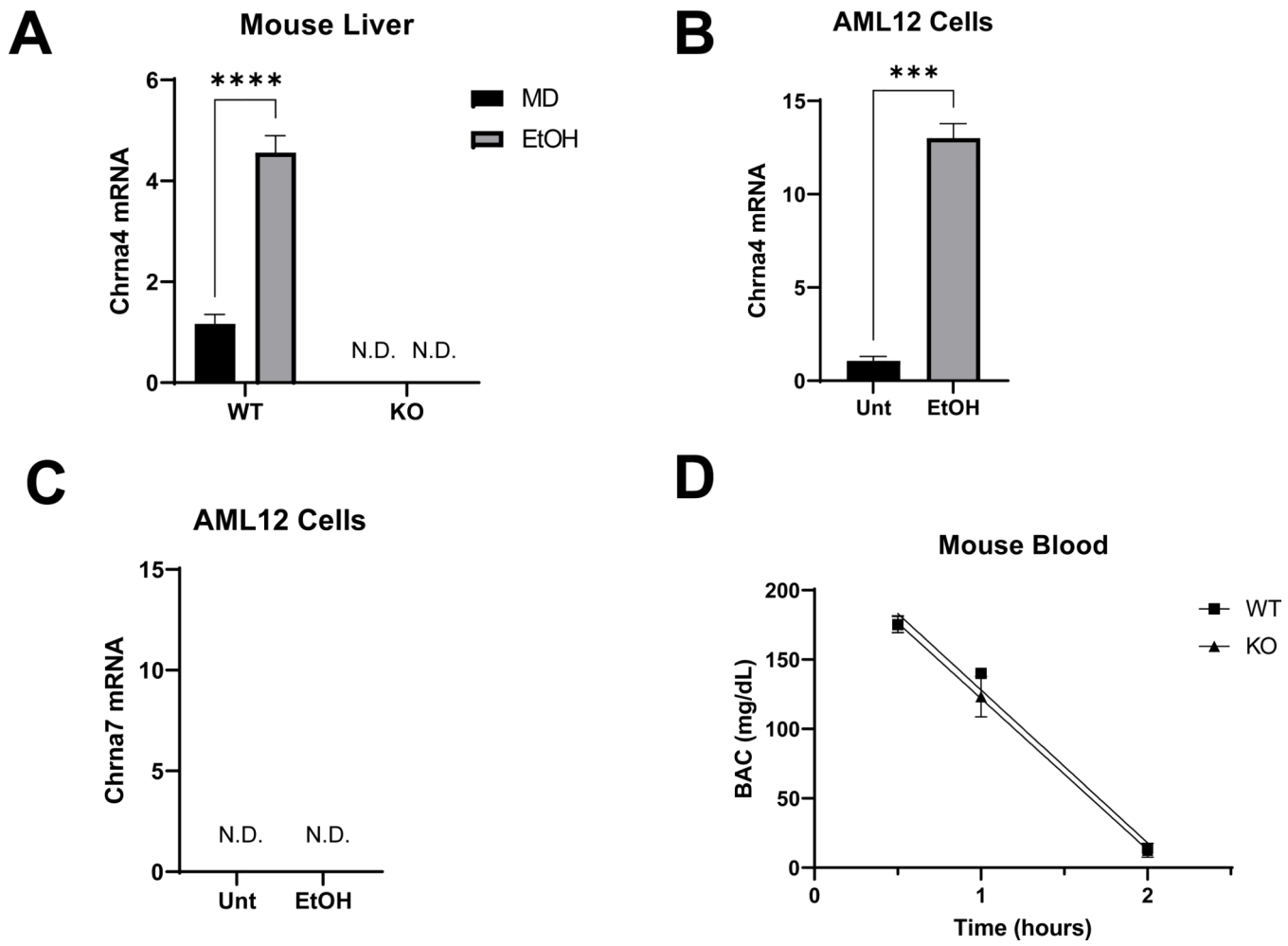

Figure 2. Alcohol induces the expression of hepatic Chrna4, and α4 KO mice metabolize alcohol normally.

(**A**) Wildtype (WT) and α4 KO mice (KO) were fed the Lieber-DeCarli alcohol diet (EtOH) or pair fed an isocaloric maltose-dextrin control diet (MD) for 6 weeks. Hepatic Chrna4 mRNA was measured by qPCR. (**B,C**) AML12 mouse hepatocytes were treated with 100 mM alcohol for 24 hours. Chrna4 (**B**) and Chrna7 (**C**) were measured by qPCR. Results of 2-Way ANOVA followed by post-hoc analysis of comparisons between groups are shown (Tukey's multiple comparisons test). Only comparisons with significant differences are indicated. The number of asterisks (*) indicates the level of significance (see Materials and Methods). (**D**) Male WT and α4 KO mice (n=5 per group) were given an i.p. injection of 1.12 g alcohol per kg body weight. Blood alcohol concentrations were determined at intervals thereafter.

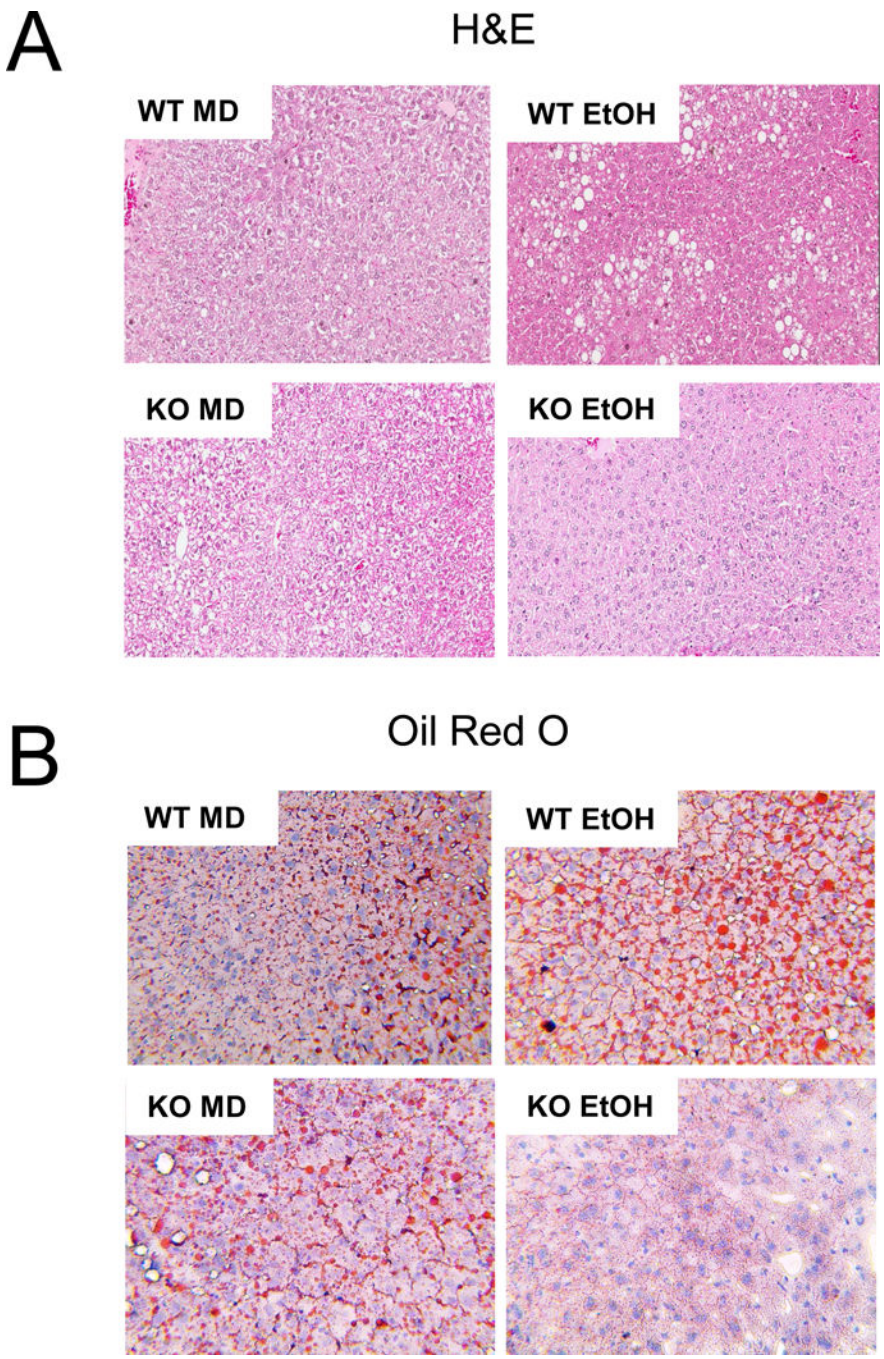

Figure 3. Alcohol exposure increases fat accumulation in the livers of wildtype but not α4 KO animals.

Wildtype (WT) and α4 KO mice (KO) were fed the Lieber-DeCarli alcohol diet (EtOH) or pair fed an isocaloric maltose-dextrin control diet (MD) for 6 weeks. (**A**) H&E staining of livers from male WT and α4 KO mice fed either the alcohol diet or the MD control diet. (**B**) Oil Red O staining of livers from male WT and KO mice fed either the alcohol diet or the MD control diet.

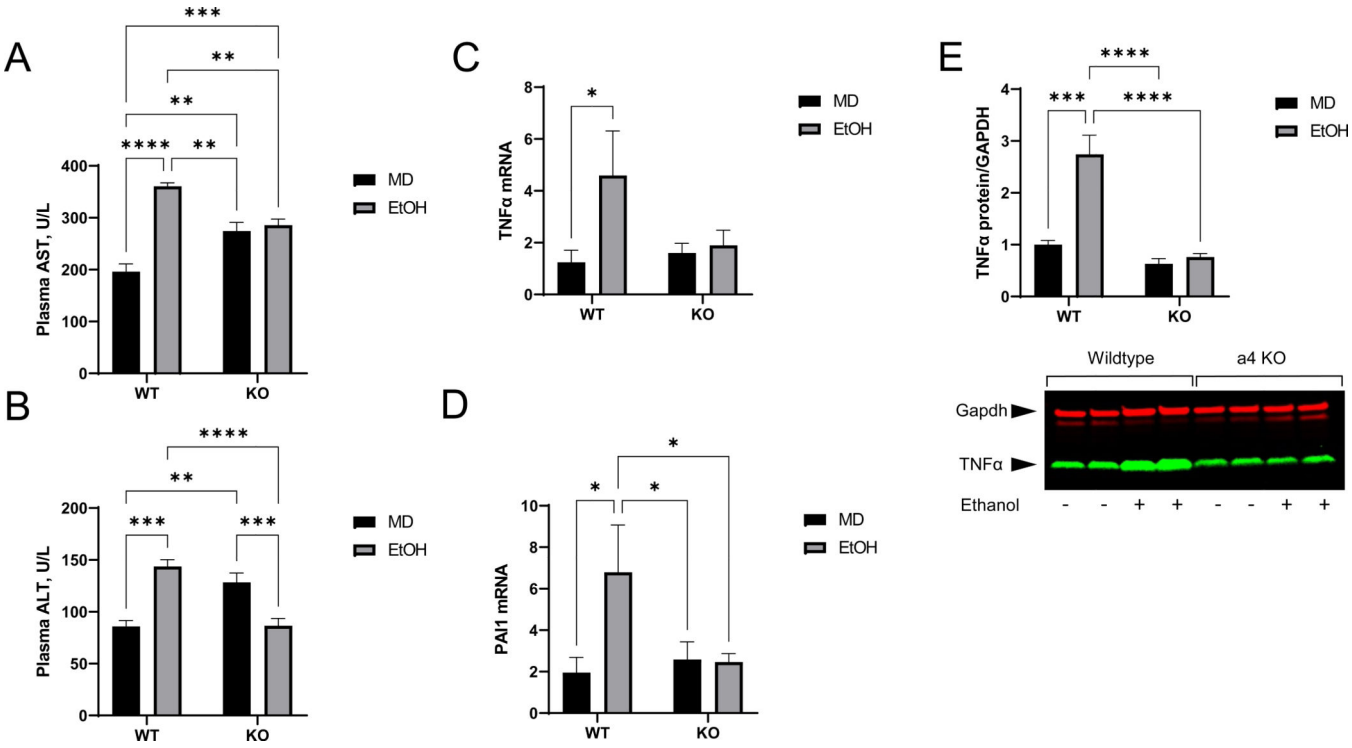

Figure 4. Alcohol exposure increases injury and inflammation in the livers of wildtype but not α4 KO animals.

WT and α4 KO male mice were fed an alcohol or MD control diet for 6 weeks, and plasma and hepatic RNA were collected. **(A)** Plasma AST and (B) plasma ALT were measured as markers of hepatocyte injury. (**C)** Hepatic TNFα mRNA and (**D**) hepatic PAI1 mRNA was measured by qPCR. **(E)** Protein levels of TNFα were measured by western blotting. Densitometric analysis is shown above the western blot image. The number of asterisks (*) indicates the level of significance by Tukey's multiple comparisons post-hoc test, as described in the Materials and Methods. Only comparisons with significant differences are indicated.

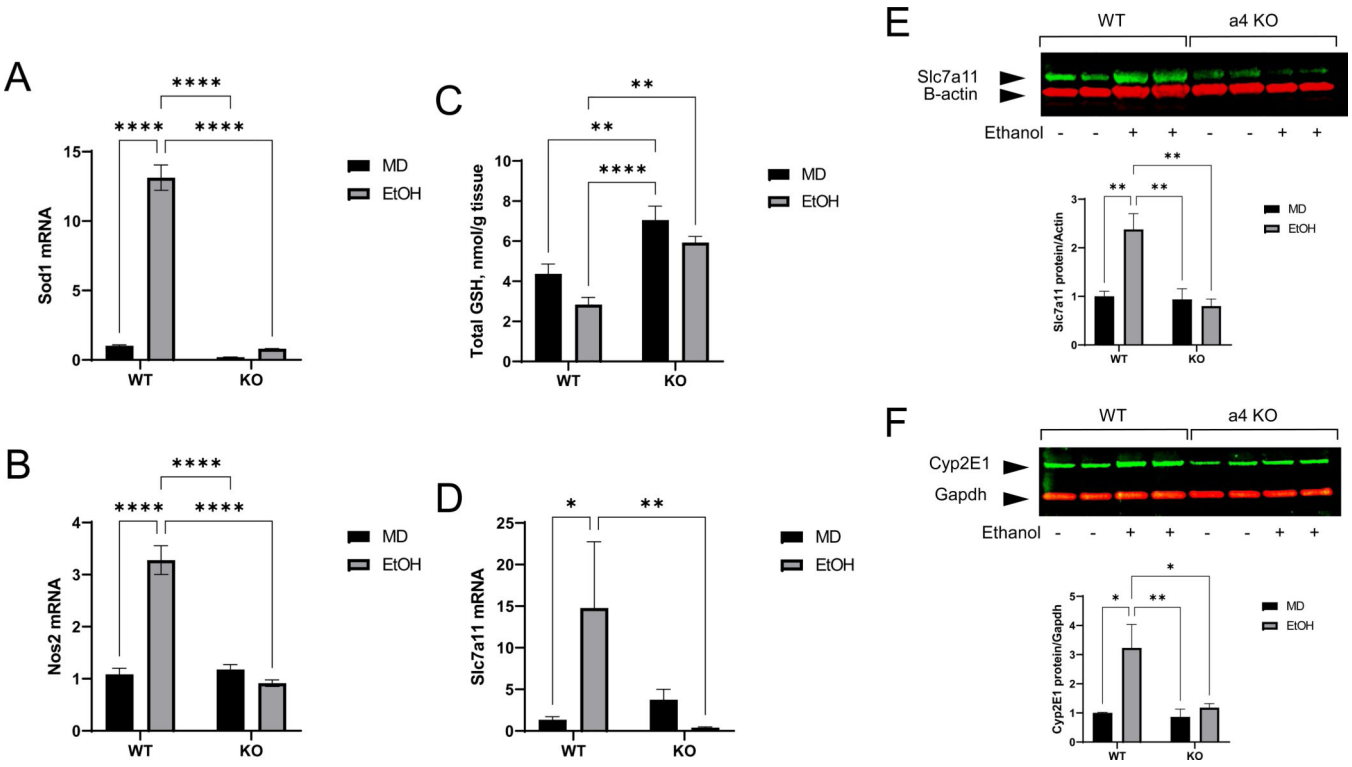

Figure 5. Markers of oxidative stress are increased in WT mice fed alcohol, but not in α4 KO mice.

Male WT and α4 KO mice were fed an alcohol or MD control diet for 6 weeks. Hepatic expression of Sod1 (**A**) and Nos2 (**B**) were measured by qPCR. (**C**) Hepatic GSH was measured by HPLC. Total GSH refers to the sum of the molar equivalents of all forms of GSH measured: GSH, GSSG and CySSG. (**D**) Hepatic expression of Slc7a11 was measured by qPCR. (**E**) Hepatic Slc7a11 protein was measured by western blotting and densitometric analysis. (**F**) Hepatic Cyp2E1 protein was measured by western blotting and densitometric analysis. Results of 2-Way ANOVA followed by post-hoc analysis of comparisons between groups are shown (Tukey's multiple comparisons test). Only comparisons with significant differences are indicated. The number of asterisks (*) indicates the level of significance (see Materials and Methods).

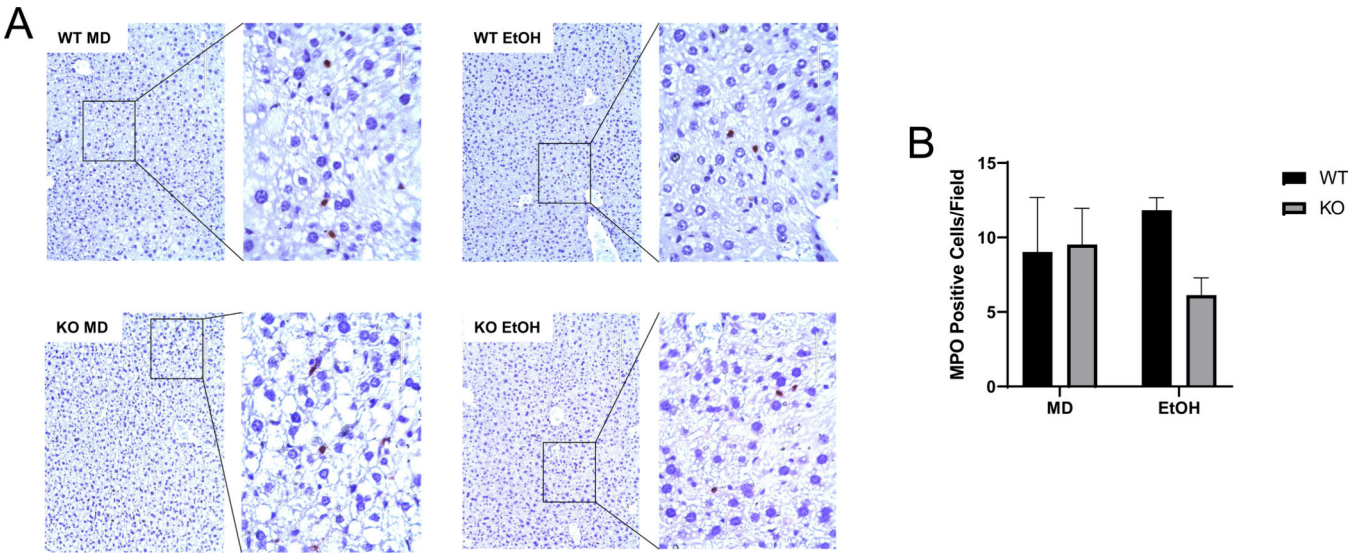

Figure 6. Alcohol exposure did not increase the number of myeloperoxidase positive cells.

(**A**) Immunohistochemical staining of myeloperoxidase in livers from male WT and α4 KO mice fed either the MD or EtOH diet. A representative field from 10 fields from each of 3 mice per group is shown. The bar in each of the wider fields taken at 20X magnification represents 200 μm. The bar in each expanded field taken at 60X magnification represents 50 μm. (**B**) The number of MPO-positive cells in each field was calculated for each mouse. The graph shows the average number of the 3 mice per group. 2-Way ANOVA indicated no significant differences.

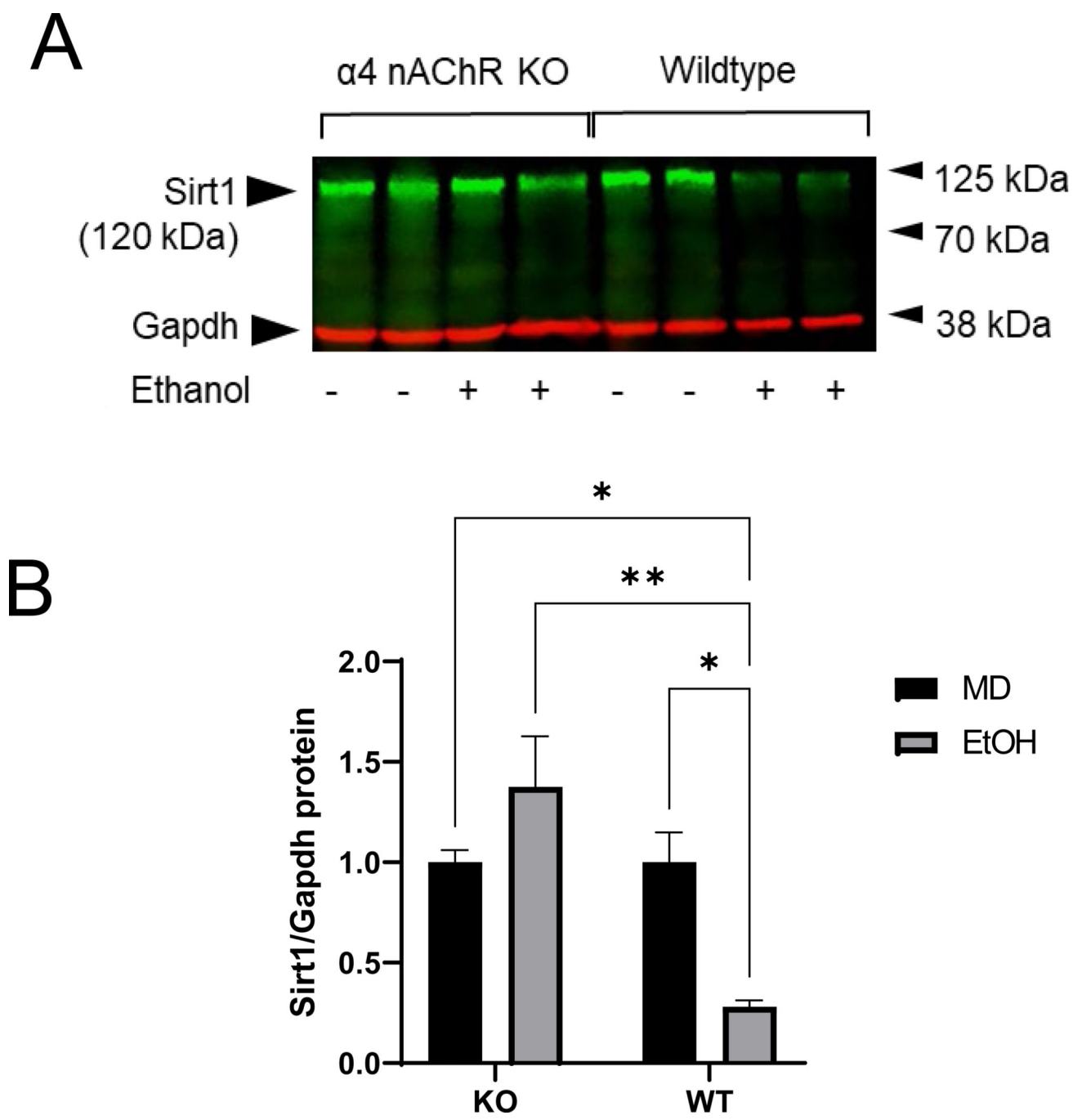

Figure 7. Alcohol exposure increases Sirt1 in the liver of wildtype but not α4 KO mice.

WT and α4 KO male mice were fed an alcohol or MD control diet for 6 weeks. (**A**) A portion of the liver was collected for western blot analysis of Sirt1. (**B)** Densitometric analysis of Sirt1 protein expression in the liver of α4 KO or WT mice exposed to alcohol compared to mice fed an isocaloric maltose-dextrin control diet. GAPDH protein levels were used for Western blot loading control and to normalize Sirt1 protein. The number of asterisks (*) indicates the level of significance by Tukey's multiple comparisons post-

hoc test, as described in the Materials and Methods. Only comparisons with significant differences are indicated.

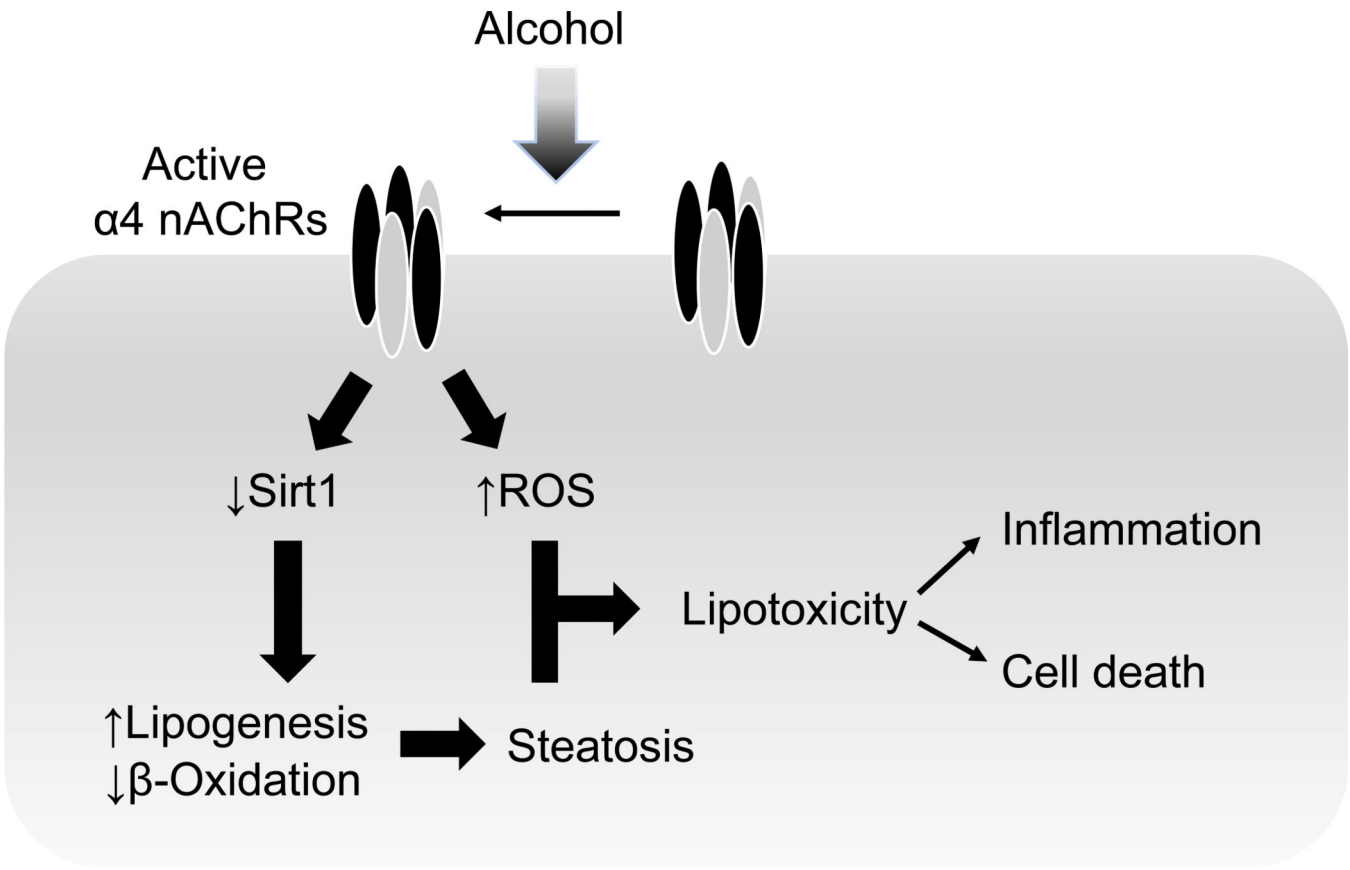

Figure 8. Scheme depicting proposed pathways by which alcohol promotes liver steatosis via α4 nAChRs.

Our data suggest that α4 nAChRs mediate alcohol-induced fat accumulation in liver through downregulation of Sirt1 which stimulates lipogenesis and decreases fatty acid β-oxidation. Steatosis in combination with reactive oxygen species (ROS) leads to inflammation and hepatocyte death. Exactly how alcohol activates α4 nAChRs is unknown, but conformational changes in the receptor caused by oxidative stress may be responsible.